ROS-stimulated protein lysine acetylation is required for crown root development in rice

Qiutao Xu, Yijie Wang, Zhengting Chen, Yaping Yue, Honglin Huang, Baoguo Wu, Yuan Liu, Dao-Xiu Zhou, Yu Zhao

Journal of Advanced Research 48 (2023) 33–46

Contents lists available at ScienceDirect

Journal of Advanced Research

journal homepage: www.elsevier.com/locate/jare

Original Article

ROS-stimulated protein lysine acetylation is required for crown root development in rice

Qiutao Xu [a,1], Yijie Wang [a,1], Zhengting Chen [a], Yaping Yue [a], Honglin Huang [a], Baoguo Wu [a], Yuan Liu [a], Dao-Xiu Zhou [a,b], Yu Zhao [a,*]

[a] National Key Laboratory of Crop Genetic Improvement, Hubei Hongshan Laboratory, Huazhong Agricultural University, 430070 Wuhan, China
[b] Institute of Plant Science Paris-Saclay (IPS2), CNRS, INRAE, University Paris–Saclay, 91405 Orsay, France

HIGHLIGHTS

- Transcription and protein levels of *PRX* genes are significantly decreased in *wox11* roots.
- Reduced ROS levels impair crown root development in rice.
- Hypo-protein acetylation levels in roots of *wox11* were caused by lower ROS levels.
- H_2O_2 application restored protein Kac levels in *wox11* roots.
- Redox regulated HDAC activity is accounted for the hypo-protein acetylation in *wox11* roots.
- This study provides new insights into the mechanism of crown root development in rice.

GRAPHICAL ABSTRACT

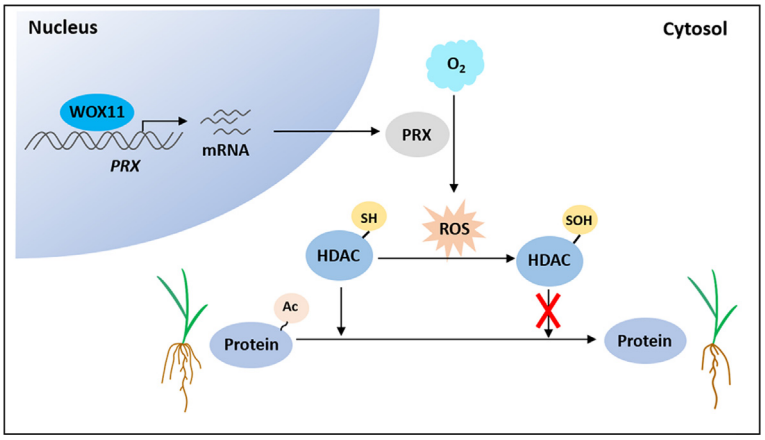

ARTICLE INFO

Article history:
Received 10 February 2022
Revised 27 June 2022
Accepted 23 July 2022
Available online 29 July 2022

Keywords:
Protein acetylation
ROS
WOX11
Proteomics
Crown roots (CRs)
Rice

ABSTRACT

Introduction: As signal molecules in aerobic organisms, locally accumulated ROS have been reported to balance cell division and differentiation in the root meristem. Protein posttranslational modifications such as lysine acetylation play critical roles in controlling a variety of cellular processes. However, the mechanism by which ROS regulate root development is unknown. In addition, how protein lysine acetylation is regulated and whether cellular ROS levels affect protein lysine acetylation remain unclear.
Objectives: We aimed to elucidate the relationship between ROS and protein acetylation by exploring a rice mutant plant that displays a decreased level of ROS in postembryonic crown root (CR) cells and severe defects in CR development.
Methods: First, proteomic analysis was used to find candidate proteins responsible for the decrease of ROS detected in the *wox11* mutant. Then, biochemical, molecular, and genetic analyses were used to study WOX11-regulated genes involved in ROS homeostasis. Finally, acetylproteomic analysis of wild type and *wox11* roots treated with or without potassium iodide (KI) and hydrogen peroxide (H_2O_2) was used to study the effects of ROS on protein acetylation in rice CR cells.
Results: We demonstrated that WOX11 was required to maintain ROS homeostasis by upregulating peroxidase genes in the crown root meristem. Acetylproteomic analysis revealed that WOX11-dependent hydrogen peroxide (H_2O_2) levels in CR cells promoted lysine acetylation of many non-histone proteins

Peer review under responsibility of Cairo University.
* Corresponding author at: Huazhong Agricultural University, No.1, Shizishan Street, Hongshan District, Wuhan, Hubei Province 430070, China.
E-mail address: zhaoyu@mail.hzau.edu.cn (Y. Zhao).
[1] These authors contributed equally to this article.

https://doi.org/10.1016/j.jare.2022.07.010

enriched for nitrogen metabolism and peptide/protein synthesis pathways. Further analysis revealed that the redox state affected histone deacetylases (HDACs) activity, which was likely related to the high levels of protein lysine acetylation in CR cells.
Conclusion: WOX11-controlled ROS level in CR meristem cells is required for protein lysine acetylation which represents a mechanism of ROS-promoted CR development in rice.

Introduction

Reactive oxygen species (ROS) are constantly generated in cells through NAD(P)H oxidases and mitochondrial electron leakage, oxidizing metabolic enzymes, and transcription factors [1,2]. As by-products of plant aerobic metabolism, ROS not only induce oxidative stress, contributing to irreversible DNA damage and cell death, but also function as signaling molecules that regulate plant growth and response to environmental stress [3]. Accumulating evidence suggests that ROS signaling is involved in a wide range of biological processes, such as enzyme activity, cell elongation, inflorescence meristem development, and abiotic stress [3–6].

In plants, root tip represents a zone of active ROS production where ROS levels are tightly and spatially regulated at cellular levels [7]. Several genetic factors were found to control ROS homeostasis in the root meristem to control root development. For instance, in *Arabidopsis*, transcription factor UPBEAT1 (UPB1) regulates the distribution of O_2^- and H_2O_2 in the root meristem and the elongation zone to promote cell division and differentiation [8]. P-loop NTPase 1 (APP1) mediates ROS homeostasis to regulate activity of the quiescent center (QC) and the distal stem cell (DSC) population, thereby maintaining the balance of stem cell division and differentiation in the root tip [9]. Root meristem Growth Factor 1 (RGF1) modulates ROS distribution to control the transition of root cell proliferation to differentiation [10]. Glutathione biosynthetic enzyme GLUTATHIONE REDUCTASE2 (GR2/MIAO) that modulates glutathione redox status is required to maintain meristem activity and root development [11]. In rice, the salicylic acid (SA) synthesis-related *aim1* (*Abnormal Inflorescence Meristem1*) mutation decreases SA content and the expression of genes involved in ROS clearance in the root tip, resulting in a shorter root phenotype [12]. In addition, environmental stresses arising from the rhizosphere that alter ROS accumulation in root cells also affect root growth. Alteration of ROS homeostasis in the root meristem due to nutrient deficiency and mechanical stresses could affect the direction and extent of root growth [13]. Hormones also play important roles in maintaining ROS homeostasis in plant roots. It was reported that auxin asymmetric distribution affects both ROS states and fine-tunes root gravitropism and hydrotropism [14]. In addition, crosstalk between NO, ROS, and auxin shapes the overall root architecture by acting in auxin signal transduction pathways [15]. However, currently there is little information regarding the molecular mechanisms by which ROS homeostasis is regulated in root meristem and how ROS affect root growth.

WOX11, a WUSCHEL-Related homeobox (WOX) family transcription factor, plays a vital role in crown root (CR) emergence and growth in rice. Loss-of-function mutation of the gene produces less and shorter CRs, whereas overexpression of *WOX11* promotes CR formation and growth and produces ectopic roots [16]. WOX11 controls CR emergence and growth by regulating the expression of cytokinin and auxin signaling genes [16,17]. Besides, WOX11 also modulates lateral root initiation, root hair formation, and abiotic stress response [16–20]. Recently, it was reported that WOX11 directly interacts with histone acetyltransferase GCN5-ADA2 module to promote the transcription of target genes to stimulate CR development [21]. ROS-related genes are overrepresented in the WOX11-activated downstream genes [22]. However, whether WOX11 controls root development by regulating ROS homeostasis remains unknown.

In this work, our results showed that WOX11 was required to maintain ROS homeostasis in CR meristem cells by activating class III peroxidases. The decrease of ROS in *wox11* mutant resulted in lysine hypo-acetylation of many proteins including those involved in protein synthesis and cell proliferation. The protein hypo-acetylation was likely due to HDACs (histone deacetylases) activities stimulated by lower ROS levels in the *wox11* roots. Our study revealed a novel pathway of WOX11-controlled CR development and provided insight into the mechanism by which ROS controls root growth and development.

Materials and methods

Plant materials and growth conditions

The 'Hwayoung' (HY) rice variety (*Oryza sativa* ssp. *japonica*) and *wox11*, which is a T-DNA insertion mutant that disrupts the *WOX11* gene in the whole plant, were used here [16]. The rice variety Zhonghua11 (ZH11) was used to generate transgenic plants. For germination, seeds of wild type and mutants were sterilized with 0.15 % $HgCl_2$. After washing with sterilized distilled water, the seeds were germinated in 1/2 MS medium with a cycle of 14 h light (28 °C)/10 h dark (24 °C). Crown roots (CRs) of HY and *wox11* (seven days old) rice seedlings were immersed in water for 4 h for pretreatment, then transferred to 1 mM KI (A100512-0250, Sangon Biotech) and 0.5 mM H_2O_2 (AR500ML, Sinopharm), respectively, for 6 h. CR tips (10 mm) with treatment were harvested for ROS, HDAC activity, and acetyl-CoA assays. For sirtinol treatment, 11-day-old rice seedlings were treated with 10 μM sirtinol for 3 days. For phenotyping, plants were grown in hydroponic culture (1.425 mM NH_4NO_3, 0.2 mM NaH_2PO_4, 0.513 mM K_2SO_4, 0.998 mM $CaCl_2$, 1.643 mM $MgSO_4$, 0.009 mM $MnCl_2$, 0.075 mM $(NH_4)_6Mo_7O_{24}$, 0.019 mM H_3BO_3, 0.155 mM $CuSO_4$, 0.152 mM $ZnSO_4$, 0.125 mM EDTA-Fe, pH 5.5) in a greenhouse with a cycle of 14 h light (28 °C)/10 h dark (24 °C). Seedlings (seven days old) were treated with 1 mM KI and 0.5 mM H_2O_2 for 7 d, by adding the chemicals directly to the hydroponic culture solution.

CRISPR/Cas9 vector construction

The design of sgRNA for the CRISPR/Cas9 system and transgenic vectors were constructed as previously described [23]. CRISPR-P2.0 [24] was used to design sgRNAs of *PRX* genes. The Cas9 and sgRNA were driven by the ubiquitin promoter and the U3/6 promoter, respectively. The sgRNA was ligated to Cas9 destination vector using the Gibson Assembly Cloning method [25]. T-DNA vectors containing Cas9 and sgRNA were transformed into rice calli. The

coding sequences (CDS) of *PRXs* from The Rice Genome Annotation Project (https://rice.uga.edu/) were amplified by PCR.

ROS, HDAC activity, and acetyl-CoA assays

For H_2O_2 assay, KI or H_2O_2-treated 7-day-old rice roots (0.1 g) were ground in liquid nitrogen, homogenized in 10 mM K-phosphate buffer (pH 6.5), and centrifuged at 12,000 rpm at 4 °C for 10 min. The supernatant was retained to measure H_2O_2 contents with H_2O_2 Quantitative Assay Kit (Sangon Biotech, C500069-0250). For detection of H_2O_2 by 3, 3-diaminobenzidine (DAB) staining, 7-day-old rice roots grown in the medium were incubated in DAB solution (1 mg/mL) for 12 h at 25 °C. H_2O_2 was detected as a brown stain and observed under a light microscope. The DAB staining intensity was analyzed by the Image J (v1.6.0_24) software.

For ROS detection, 7-day-old rice CR tips grown in the medium were incubated in 10 μM 2, 7-dichlorodihydrofluorescein diacetate (H_2DCFDA, dissolved in 10 mM K-phosphate buffer, pH 6.5) at 25 ℃ for 2 h. Then, the CRs were rinsed with 10 mM K-phosphate buffer (pH 6.5) to remove H_2DCFDA from the surface of CRs. The relative H_2DCFDA staining intensity was analyzed by Image J (v1.6.0_24) software.

For HDAC enzyme activity assay, KI or H_2O_2-treated 7-day-old rice CR tip samples (0.1 g) were ground into powder with liquid nitrogen, and suspended in 500 μL protein extraction buffer (62.5 mM Tris-HCl, pH 6.8). After centrifugation at 16,000 g for 15 min at 4 °C, the supernatants were collected. Protein concentrations were determined using Protein Quantification Kit (Vazyme Biotech, E211-01). HDAC activities were measured with the HDAC Activity/Inhibition Assay Kit (EpiGentek, P-4035–96). Briefly, the protein samples (10 μg) and the substrate were incubated at 37 °C for 60–90 min, then the capture antibody was added and incubated at 25 °C for 60 min, followed by the addition of detection antibody and incubation for 30 min. Finally, the fluorescent developer was added and incubated for 2–4 min at room temperature in a $530_{EX}/590_{EM}$ fluorescent microplate instrument (Tecan Infinite 1000) to measure the deacetylation product.

Acetyl-CoA contents were measured as previously reported [26]. Briefly, KI or H_2O_2-treated 7-day-old rice CR tips (0.1 g) were ground in liquid nitrogen and suspended in 0.9 mL of PBS (pH 7.0). The suspensions were vortexed and placed at 25 °C for 20 min and centrifuged at 16,873 g for 15 min at 4 °C. The supernatants were collected for acetyl-CoA content measurement using an acetyl-CoA assay kit (Ji Ning Biotech, China, JN709212).

Biochemical analysis of protein redox status

Rice seedlings, overexpression lines (OE) fused with FLAG tag at C-terminal of SRT1, SRT2, HDA710, and HDA714, were grown in 1/2 MS medium with a cycle of 14 h light (28 °C)/10 h dark (24 °C). For the redox treatment, seedlings were first immersed in water for 4 h for pretreatment and then transferred to 1 mM KI or 0.5 mM H_2O_2 for 6 h. Then CRs were collected. The redox status of proteins was determined as previously reported with minor modifications [27,28]. Briefly, samples of 0.2 g rice CRs were ground into powder with liquid nitrogen and suspended in 300 μL of protein extraction buffer (62.5 mM Tris-HCl, pH 6.8; 2 % (w/v) SDS). The samples were centrifuged at 16,000 g for 15 min at 4 °C. The supernatants were collected and proteins were precipitated with 10 % TCA-acetone at −20 °C for 12 h. The TCA precipitates were collected by centrifugation at 16,000 g for 15 min at 4 °C. After washing twice with pre-cooled acetone, the protein pellets were dissolved in 100 μL of thiol labeling solution (62.5 mM Tris-HCl, pH 6.8; 2 % [w/v] SDS; 0.04 % [w/v] Bromophenol Blue [BPB]; 16 mM 4-acetamido-4′ -maleimidylstilbene-2, 2′-disulfonic acid [AMS]) and kept in the dark at 25 °C for 1 h to allow AMS to react with free thiol groups. The samples were boiled for 10 min at 90 °C and analyzed by Western blotting.

RNA extraction and qPCR analysis

Total RNA was extracted from CR tips by TRIzol reagent (Invitrogen) following the manufacturer's instructions. HiScript II Q RT SuperMix for qPCR kit (Vazyme Biotech, R223-01) was used for reverse transcription. For qPCR analysis, 2.5 μL of primers, 2.5 μL of cDNA template and 5 μL of 2 × SYBR Mix (Vazyme Biotech, Q712-02) were added. Reactions were carried out on a qPCR machine (Applied Biosystems). The internal control gene was *ACTIN1*. Three independent biological replicates were performed. The primer sequences used are listed in Supplementary Table S1.

Electrophoretic mobility shift assay

To produce the WOX11 protein, the full-length cDNA was inserted into PET28A expression vector (GE Healthcare) and expressed in *Escherichia coli* DE3 (BL21) cells (GE Healthcare). The target protein was purified with Ni-NTA Agarose (Qiagen, Alameda, CA) according to the manufacturer's instruction. The oligonucleotides of *PRXs* with the putative WOX11 binding site (TTAATGG/C) were synthesized and labeled with 5'-biotin by the Sangon Biotech Company (Shanghai, China). Double-stranded oligonucleotides were produced by mixing equal amounts of complementary single-stranded oligonucleotides at 95 °C for 2 min, followed by gradual cooling from 72 °C to room temperature for annealing. DNA binding reactions were performed in the presence or absence of unlabeled *PRXs* fragments at different molar excess at room temperature for 20 min in 10 mM Tris, pH 7.5, 50 mM NaCl, 1 mM DTT, 1 mM EDTA, 1 mM $MgCl_2$, 5 % glycerol, and 50 mg/L poly (dI-dC) (Amersham Pharmacia Biotech). The final reactions were run on a 6 % polyacrylamide gel in Tris-glycine (0.3 % Tris and 1.88 % glycine) buffer and detected by a chemiluminescent imaging system (Tanon 5200).

Dual-luciferase assay

PRX111 promoter (-1000 to + 100 bp relative to the ATG codon) amplified from ZH11 (wild type) plants were used to drive the reporter gene expression. The mutant versions of the promoter were obtained by PCR-based site-directed mutagenesis. *WOX11* CDS driven by the 35S promoter was ligated to Effector vector. The effector and reporter constructs together with the control vector were co-transfected into protoplasts at the 6:6:1 ratio. The transfected protoplasts were placed in the dark at room temperature overnight. The protoplasts were collected by centrifugation in 1.5 mL tubes at 100 g for 8 min at room temperature. The activities of luciferase were determined according to the kit instructions (Promega, E1910). Briefly, 50 μL of lysis buffer (1 ×) was added to the pelleted protoplasts. After centrifugation at 12,000 rpm for 5 min, the supernatant (40 μL) was transferred to a 96-well enzyme plate (COSTAR 3917 Assay Plate, 96 Well, Lot NO: 04313012) containing 50 μL of Kit A. The fluorescence signal intensity on ELISA (TECAN infinite M200) was measured. Then 50 μL of Kit B was added and the fluorescence signal was detected again. The relative expression level of the reporter genes was detected as the ratio of the relative value of firefly LUC to that of Renilla luciferase.

Chromatin immunoprecipitation (ChIP)-qPCR

ChIP experiment was carried out as previously described [29]. Briefly, rice CR tips (1 g) were cross-linked in 1 % formaldehyde

(F8775, Sigma-Aldrich) for 30 min, ground into powder in liquid nitrogen, and extracted with the lysis buffer (10 mM Tris-HCl, pH 8.0, 0.4 M sucrose, 0.1 mM phenylmethylsulfonyl fluoride [PMSF], 10 mM $MgCl_2$, 5 mM β-mercaptoethanol, 1 protease inhibitor cocktail). Next, the mixture was cleaned by filtering through a double layer of Miracloth (Millipore) and centrifuged at 4,000 g at 4 °C for 20 min. The final chromatin precipitation was washed at least five times with washing buffer (0.25 M sucrose, 10 mM Tris, pH 8.0, 1 % Triton X-100, 10 mM $MgCl_2$, 0.1 mM PMSF, 5 mM β-mercaptoethanol, 1 protease inhibitor cocktail) and suspended with 300 μL of nucleus lysis buffer (50 mM Tris-HCl, pH 8.0, 10 mM EDTA, 1 % [w/v] SDS). Then chromatin was sonicated to 200–500 bp (20 μL of sonicated chromatin were taken out as input) and immune-precipitated with the anti-WOX11 (5 μg, antigen used was the full length of WOX11 protein) antibody [29]. The immunoprecipitated chromatin was washed sequentially with following buffer: low salt buffer (150 mM NaCl, 50 mM HEPES-KOH, 1 mM EDTA, 0.1 % sodium deoxycholate, 1 % Triton X-100, 0.1 % SDS), high salt buffer (same to low salt buffer except using 350 mM NaCl), LiCl buffer (10 mM Tris-HCl pH 8.0, 0.5 % NP-40, 250 mM LiCl, 0.1 % sodium deoxycholate, 1 mM EDTA) and TE buffer (1 mM EDTA, 10 mM Tris-HCl, pH 8.0), and eluted with elution buffer (10 mM EDTA, 50 mM Tris-HCl, pH 7.5, 1 % SDS) at 65 °C for 15 min with shaking (800 rpm). The elutes were reverse-crosslinked with 5 M NaCl at 65 °C overnight, purified with chloroform, and precipitated with alcohol. The input and precipitated DNA fragments were checked by RT-qPCR using primers listed in Supplementary Table S1. Three independent biological replicates were performed.

Protein extraction and immunoblotting

Protein extraction was performed as previously reported [30–32]. Briefly, rice CRs were ground in liquid nitrogen and suspended in the extraction buffer (10 mM EGTA, pH 7.5, 1 % [v/v] TritonX-100, 10 mM Tris-HCl, 1 mM PMSF, 1 mM DTT, and 250 mM sucrose). The samples were centrifuged at 15,000 g for 15 min at 4 °C and precipitated with cold acetone at −20 °C for 2 h. Protein pellets were collected by 15,000 g centrifugation at 4 °C for 15 min and the precipitates were washed three times with cold acetone, lyophilized, and stored at −80 °C.

Immunoblotting was performed as previously reported [33]. Briefly, proteins were separated by 10–12 % SDS-PAGE gel and transferred onto a PVDF membrane. The final blot was detected by anti-acetylated lysine antibody (1:1000, PTM-102, PTM Biolab).

LC-MS/MS-based quantitative acetylproteomics

Acetylproteomics of sirtinol-treated plants was performed as previously reported [34]. Following are the basic steps of root acetylproteomic analysis:

Trypsin digestion

First, the protein solution was reduced with 5 mM dithiothreitol at 56 °C for 30 min, then alkylated with 11 mM iodoacetamide at 25 °C for 15 min in darkness. The urea concentration of the protein sample was diluted to < 2 M by adding 100 mM TEAB. Finally, trypsin was added at the 1:50 ratio (trypsin/protein in mass) for the first-round digestion (12 h) and 1:100 for second-round digestion (4 h).

Affinity enrichment

The peptides were dissolved in IP buffer solution (100 mM NaCl, 50 mM Tris-HCl, 1 mM EDTA, 0.5 % NP-40, pH 8.0) containing the antibody beads (PTM-104, PTM Bio) and gently mixed at 4 °C for 12 h. After incubation, the beads were washed with the IP buffer four times and then with deionized water 2 times. Finally, the peptides were eluted three times with 0.1 % trifluoroacetic acid and collected and dried by vacuum. For LC-MS/MS analysis, the peptides were desalted with C18 ZipTips (Millipore) following the manufacturer's instructions.

LC-MS/MS analysis

The peptides were dissolved in a mobile phase A and separated by a NanoElute ultra performance liquid chromatography system. Mobile phase A was 0.1 % formic acid. Mobile phase B was 0.1 % formic acid in acetonitrile solution. Gradient setting for liquid phase was as follows: 0–20 min, 6 %–22 % B; 20–26 min, 22 %-30 % B; 26–28 min, 30 %-80 % B; 28–30 min, 80 % B; maintaining flow rate was set at 300 nL/min.

The peptides were first separated by ultra-performance liquid chromatography and then ionized by the Capillary ion source. Next, the peptides were analyzed with a TIMS-TOF Pro mass spectrometry. Ion source voltage was set at 1.4 kV. TOF was used to detect the secondary fragments and peptide parent ions. The secondary mass spectrometry scanning range was set at 100–1700 *m/z*. The parallel cumulative serial fragmentation (PASEF) mode was used for the data acquisition mode. A secondary spectrogram was collected with the charge of the parent ion in the range of 0–5 in PASEF mode 10 times when the first-stage mass spectrometry acquisition was done. The tandem mass spectrometry scanning elimination time was 24 s to avoid the repetitive scanning of the parent ion.

Database search

The resulting MS/MS data were analyzed by Maxquant (v1.6.6.0). *Oryza_sativa_japonica*_UniPort (48914 proteins) database, the anti-database, and common contamination database were added to calculate the false positive rate (FDR), and to avoid contaminated proteins influence, respectively; The enzyme digestion mode was set to Trypsin/P and the number of missing sites was set to 4. The mass error tolerance of the primary parent ion of First search and Main search was set to 70 ppm and the mass error tolerance of the secondary fragment ion was 0.04 Da. The alkylation of cysteine was set as fixed modification; methionine oxidation, *N*-terminal acetylation of protein, acetylation of lysine, and deamidation were set as variable modifications. The FDR values < 1 % of PSM and protein identification were selected.

Bioinformatic data analysis

Gene ontology analysis was based on AgriGo (v2.0) [35]. Heatmaps were generated by TBtools (v0.6) [36]. Kac motif analysis was analyzed by the iceLogo motif builder [37] with a p-value of 0.05. Ridge plots and scatter plots were generated in R (v3.5). Protein quantification was performed separately for each replicate to identify up and downregulated proteins. Only those proteins that showed > 1.5/2-fold changes in both replicates (relative to wild type) were considered as significantly regulated.

Results

The abundance of proteins involved in ROS production is decreased in wox11 mutant roots

Transcriptomic analysis of *wox11* mutant roots revealed that the expression levels of redox-related genes were dramatically

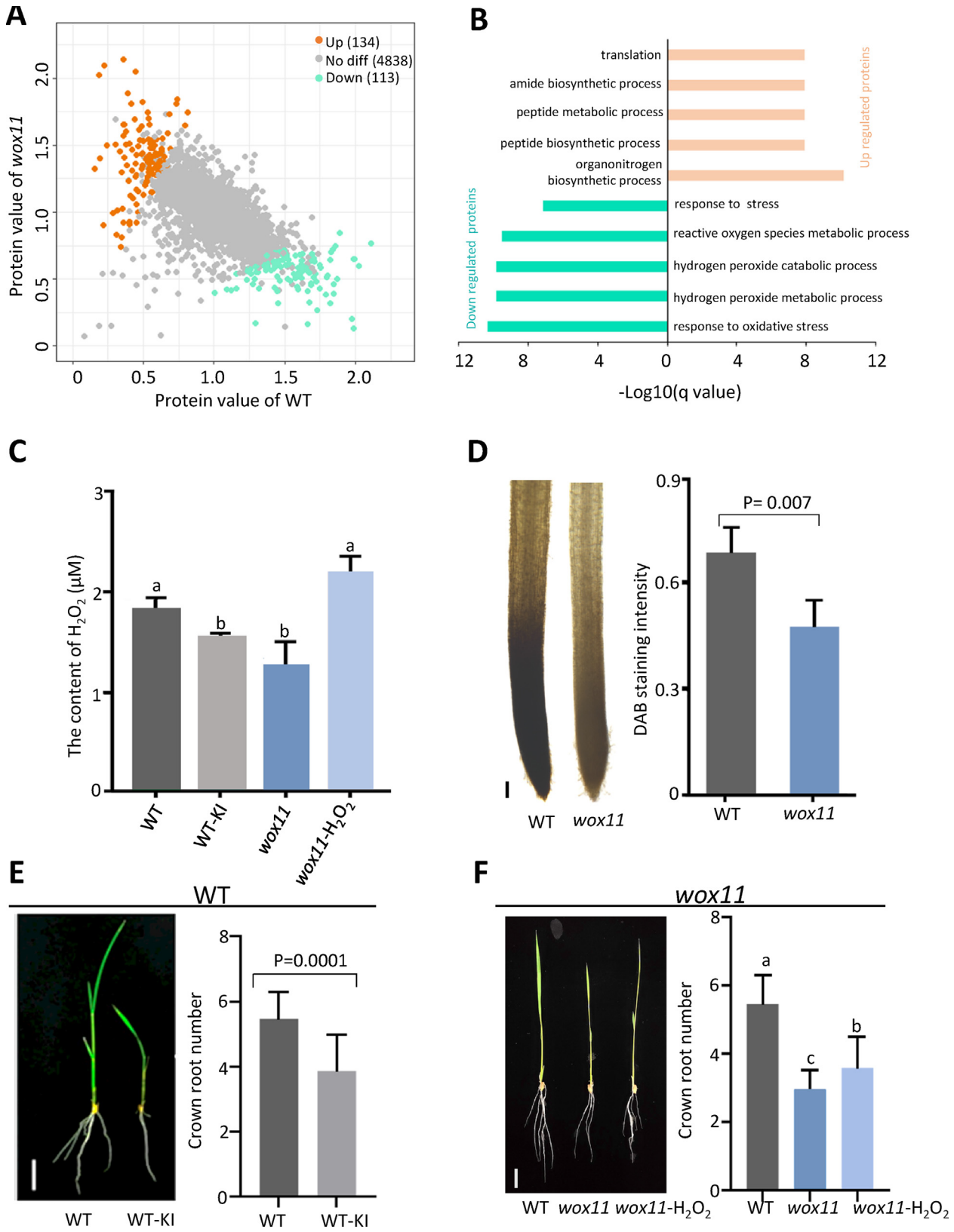

Fig. 1. WOX11 is involved in ROS level for crown root growth. (A) Significantly upregulated (N = 134, fold change > 2) and downregulated proteins (N = 113, fold change > 2) in *wox11* versus wild type (WT) crown roots. **(B)** GO pathway enrichment analysis of proteins with significant changes in *wox11* crown roots. **(C)** H_2O_2 content assay in crown roots of WT, WT-KI (wild type plants treated by KI), *wox11*, and *wox11*-H_2O_2 (*wox11* treated by H_2O_2) plants. Error bars represent means ± SD (n = 3) from three biological replicates. **(D)** Detection of H_2O_2 accumulation in WT and *wox11* crown roots by DAB staining. Error bars are means ± SD (n = 10) from three biological replicates. Bar = 100 μm. DAB staining intensities were analyzed by Image J software. **(E, F)** Crown root phenotypes of WT, WT-KI, *wox11*, and *wox11*-H_2O_2 plants. Error bars are means ± SD (n = 15) from three biological replicates. Bar = 2 cm. The significant difference in D and E was calculated by the two-tailed Student *t*-test. In C and F, significance was calculated using one-way ANOVA with Tukey's multiple comparison test. Different letters on top of the bars indicate significant differences (P < 0.05), and the same letters on top of bars indicate no significant difference (C, F).

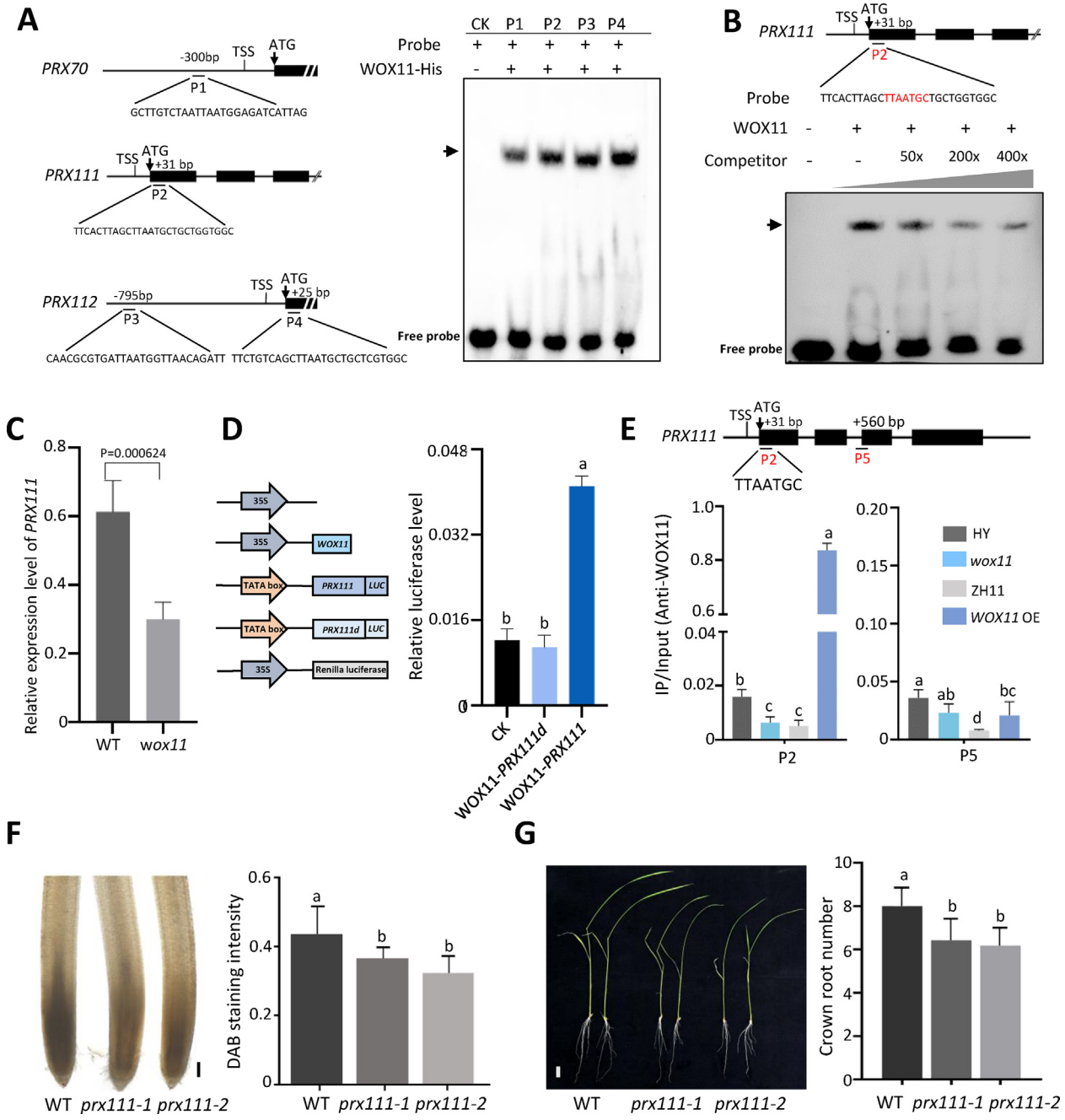

Fig. 2. WOX11 stimulates ROS production in roots by directly activating *PRX111*. **(A)** Electrophoretic mobility shift assays (EMSA) showing that *E.coli*-produced WOX11 directly binds to the TTAATGG/C motif in *PRXs*. Left, DNA sequence of the probes used in EMSA. Right, EMSA. Arrow indicated WOX11 protein and biotin-labeled DNA complex. CK denotes the reaction without WOX11-His protein. P1 to P4 are sequences which contain WOX11 binding site. **(B)** Electrophoretic mobility shift assay (EMSA) of WOX11 protein binding to the TTAATGC motif (WOX11-binding site) within *PRX111* gene body. *E. coli*-produced WOX11 protein was incubated with 5′-biotin-labeled P2 in the absence or presence of 50, 200 or 400 M excess of the corresponding cold probes and analyzed by electrophoresis. The shifted band is indicated by the arrow. Three biological replicates were conducted. **(C)** Expression level of *PRX111* in *wox11* and wild type (WT). The $2^{-\triangle\triangle ct}$ method was used for the quantification of relative expression. The PCR signals were normalized with those of the *ACTIN1* transcripts. Error bars are means ± SD (n = 3) from three biological replicates. **(D)** Dual-luciferase assay of WOX11 activating *PRX111* expression in rice protoplasts. The promoter (1 kb upstream ATG) plus 100 bp downstream of ATG of *PRX111* was used. *PRX111d* refers to the 1.1 kb *PRX111* sequence with deleted TTAATGC motif. **(E)** ChIP-qPCR analysis of *in vivo* binding of WOX11 to the *PRX111*. Upper panel: Schematic representation of one putative locus of WOX11 binding sites in the *PRX111* genomic sequence. P2 (31 bp from ATG) including TTAATGC motif, P5 (560 bp from ATG) without TTAATGC motif; TSS, transcription start site; ATG, translation start site. Lower panel: Nuclei from wild type (ZH11, HY), *wox11*, and WOX11 overexpression (*WOX11* OE) crown roots were immunoprecipitated with anti-WOX11. *wox11* and WOX11 OE were in HY and ZH11 backgrounds, respectively. The precipitated chromatin fragments were analyzed by qPCR using two primer sets amplifying two *PRX111* regions (P2, and P5) as indicated in upper panel. Error bars represented the means ± SD (n = 3) from three biological replicates. **(F)** Detection of H_2O_2 accumulation in WT and *prx111* crown roots by DAB staining. Error bars were means ± SD (n = 10) from three biological replicates. Bar = 100 μm. DAB staining was evaluated by measuring intensity level with Image J software. **(G)** The phenotype of wild type (WT) and *prx111* seedling crown roots. Error bars were means ± SD (n = 12) from three biological replicates. Bar = 1 cm. The significant difference in C was calculated by the two-tailed Student *t*-test. While in D-G, significance was calculated using one-way ANOVA with Tukey's multiple comparison test. Different letters on top of the bars indicate significant differences ($P < 0.05$), and the same letters on top of bars indicate no significant difference (D-G).

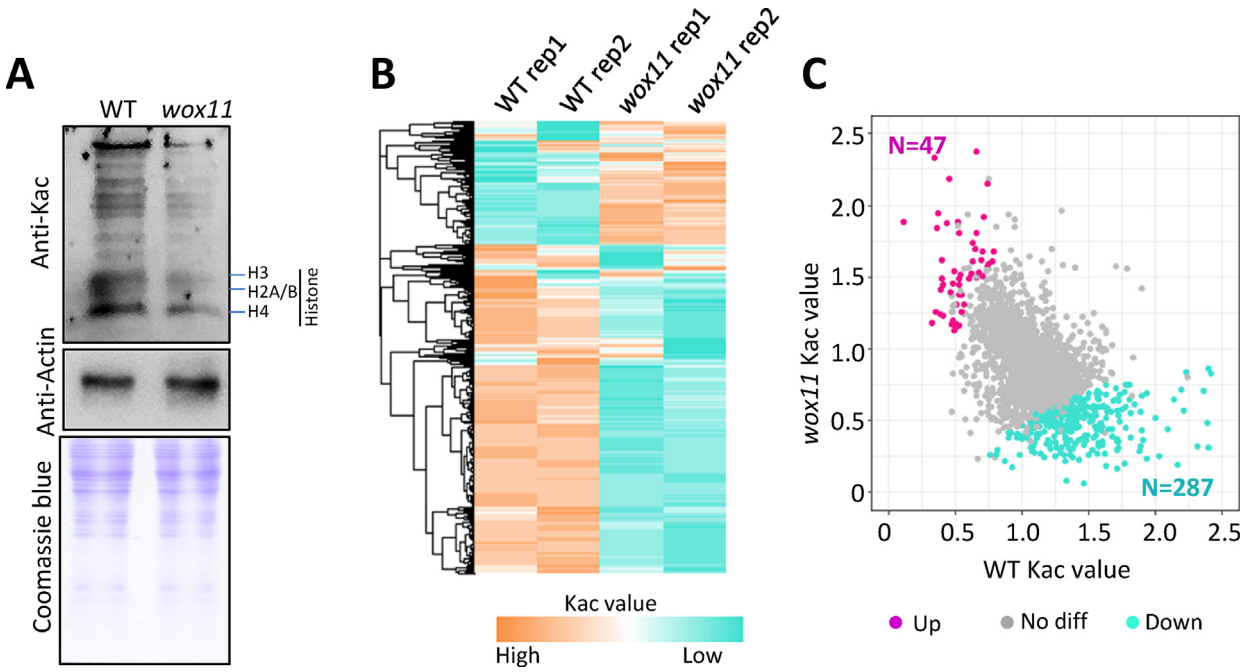

Fig. 3. The *wox11* mutation leads to protein hypo-acetylation in crown roots. **(A)** Immunoblotting detection of Kac level in WT and *wox11* crown roots with lysine acetylation antibody. Immunoblotting with anti-actin antibody and Coomassie blue staining were used as loading control. **(B)** Heatmap showing proteins Kac levels in WT and *wox11* crown roots. **(C)** Scattering plots of acetylation levels at individual Kac sites between wild type and *wox11*. Significantly up (N = 47, fold change > 2) and downregulated sites (N = 287, fold change > 2) in the mutants are indicated by purple and green, respectively.

decreased in the mutant [22]. To study whether the differential expression of the genes eventually affected their protein abundance in the mutant, proteomic profiling by mass spectrometry (MS) (two biological replicates) was carried out on the root tissues similar to those used for the transcriptome profiling. We assessed the reproducibility of the biological replicates of the proteome by calculating Pearson correlations and found an average of 0.79 (Figure S1A). Totally, 7,193 proteins were identified in wild-type (WT) rice roots (Supplementary Table S2), with nearly all proteins matched with the 25,061 transcripts of transcriptome data (Figure S1B). The proteome displayed some correlation (Pearson r = 0.55) with the transcriptome (Figure S1C). In addition, the proteins identified by MS corresponded to the high-abundance population of transcripts with an average TPM (transcript per million) > 97.80 (Figure S1D). Importantly, in the root proteome, we identified 130 ROS homeostasis-related proteins including 79 Class III peroxidases (PRXs) (representing about 57 % of all peroxidase genes in the rice genome), 30 thioredoxins, 7 ascorbate peroxidases, 5 superoxide dismutases, 4 glutathione peroxidases, 3 catalases, and 2 RBOHs (Respiratory Burst Oxidase Homolog H). Most of the genes displayed a root-specific expression pattern (Figure S2A). In *wox11* roots, 113 and 134 proteins were down and upregulated (> 2 folds), respectively (Fig. 1A, Supplementary Table S3). The downregulated proteins were enriched for oxidative stress response and ROS/hydrogen peroxide metabolisms, while upregulated proteins were enriched for protein synthesis-related pathways (Fig. 1B). In particular, both the transcript and protein levels of 5 peroxidases showed consistent downregulation between transcriptome and proteome of *wox11* roots (Figure S2B). Three of the 5 *PRX* genes contained the WOX11-binding motif at their promoters (1 kb upstream to ATG) or gene bodies (Figure S2B). The analysis indicates that the root transcriptome and proteome are correlated and that proteins involved in cellular ROS homeostasis are accumulated in roots. The *wox11* mutation affected their accumulation.

WOX11-regulated ROS is required for CR development

To evaluate H_2O_2 and ROS levels in *wox11* roots, we performed H_2O_2 quantitative assays, 3, 3′-diaminobenzidine (DAB) and 2, 7-dichlorodihydrofluorescein diacetate (H_2DCFDA) assays. The analysis revealed that ROS levels were greatly decreased in *wox11* roots compared with WT (Fig. 1C, D, S3B). To study whether the WOX11-dependent ROS levels were required for root growth, we treated *wox11* roots with hydrogen peroxide (H_2O_2) and WT roots with potassium iodide (KI, a general H_2O_2 scavenger), and investigated their effects on CR development. H_2O_2 content assays confirmed that the application of KI and H_2O_2 altered the H_2O_2 levels in WT and *wox11* roots (Fig. 1C). The H_2O_2 level in WT roots treated with KI (WT-KI) was clearly decreased compared with control (Fig. 1C) and the CR number of WT-KI was similar to that of *wox11* roots (Fig. 1E). In contrast, H_2O_2 application increased the CR number of *wox11* plants (Fig. 1F). Together, these results suggest that WOX11 might maintain ROS levels in crown roots by regulating the expression of genes involved in ROS production.

To study whether WOX11 directly regulated the expression of ROS-related genes, we performed EMSA experiments and found that WOX11 bound *in vitro* to the three *PRX* genes (*PRX70*, *PRX111*, and *PRX112*) which contained the WOX11 binding site TTAATGG/C within the promoters or gene bodies (Fig. 2A, B, Figure S2B). Among the three *PRX* genes, we selected *PRX111* for further study, because both its mRNA and protein levels showed clear decreases in *wox11* roots (Figure S2B). RT-qPCR assay also confirmed the downregulation of *PRX111* transcript in *wox11* roots (Fig. 2C). Dual-luciferase reporter assays showed that WOX11 binding was required for *PRX111* expression in rice cells (Fig. 2D). Furthermore, chromatin immunoprecipitation (ChIP) analysis revealed *in vivo* interaction of WOX11 with *PRX111* (Fig. 2E). To investigate whether *PRX111* was required for ROS production and CR development, we produced *prx111* knockout plants by using the CRISPR/Cas9 technology (Figure S3A). The *prx111* knockout

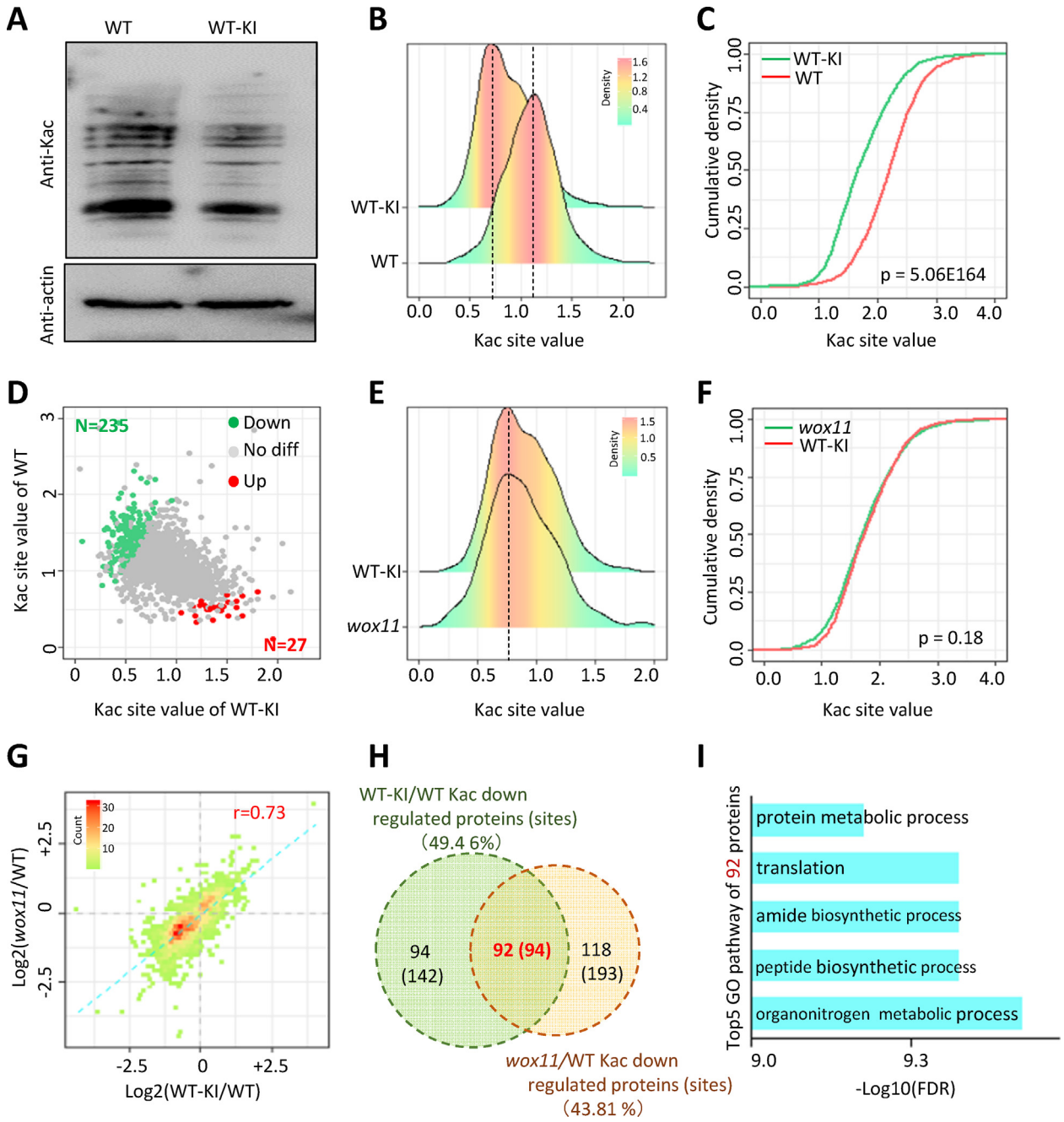

Fig. 4. Decreased ROS contents lead to hypo-Kac in *wox11* crown roots. (A) Immunoblotting detection of Kac levels with lysine acetylation antibody in crown roots of WT and WT-KI. Immunoblotting with anti-actin antibody was used as loading control. **(B)** Ridge plots of acetylation levels at individual Kac sites in WT-KI and WT crown roots. **(C)** Cumulative density plots of the acetylation levels at individual Kac sites in WT-KI and WT crown roots. **(D)** Scattering plot of proteins with significantly upregulated (N = 27, fold change > 2) and downregulated (N = 235, fold change > 2) acetylation levels at individual Kac sites in WT-KI versus WT crown roots. **(E)** Ridge plots showing acetylation levels at individual Kac sites in WT-KI and *wox11* roots. **(F)** Cumulative density plots of the Kac site values in WT-KI and *wox11* crown roots. P value in C and F was calculated by a two-tailed Student *t*-test. **(G)** Correlation between Kac changes in WT-KI/WT and *wox11*/WT. Pearson correlation (r = 0.73) was shown. **(H)** Overlap between proteins (sites) with significant downregulated Kac levels in WT-KI/WT and *wox11*/WT. **(I)** GO pathway enrichment analysis of 92 overlapped proteins in H.

plants showed reduced root ROS levels (Fig. 2F, S3C) and produced fewer CR, phenocopying that of *wox11* mutant (Fig. 2G). Collectively, these results support the idea that the WOX11-regulated ROS homeostasis is required for CR development.

The wox11 mutation results in protein hypo-acetylation in roots

ROS accumulation often affects protein posttranslational modifications (PTM) [31]. To study whether the lower ROS levels in *wox11* impacted overall protein lysine acetylation in roots, we performed immunoblotting analysis and found that in addition to histones, Kac level of non-histone proteins in *wox11* was clearly decreased (Fig. 3A). To identify proteins whose Kac levels were altered in *wox11* roots, quantitative acetylproteomic analysis was performed. The *wox11* and WT root samples were similar to those used for transcriptomic and proteomic investigations. To avoid any bias that might be caused by variation in protein abundance, we calibrated the acetylation levels relative to that of the proteins (Supplementary Table S2). The data obtained from the two biological replicates were highly correlated (Figure S4). About half (49 %)

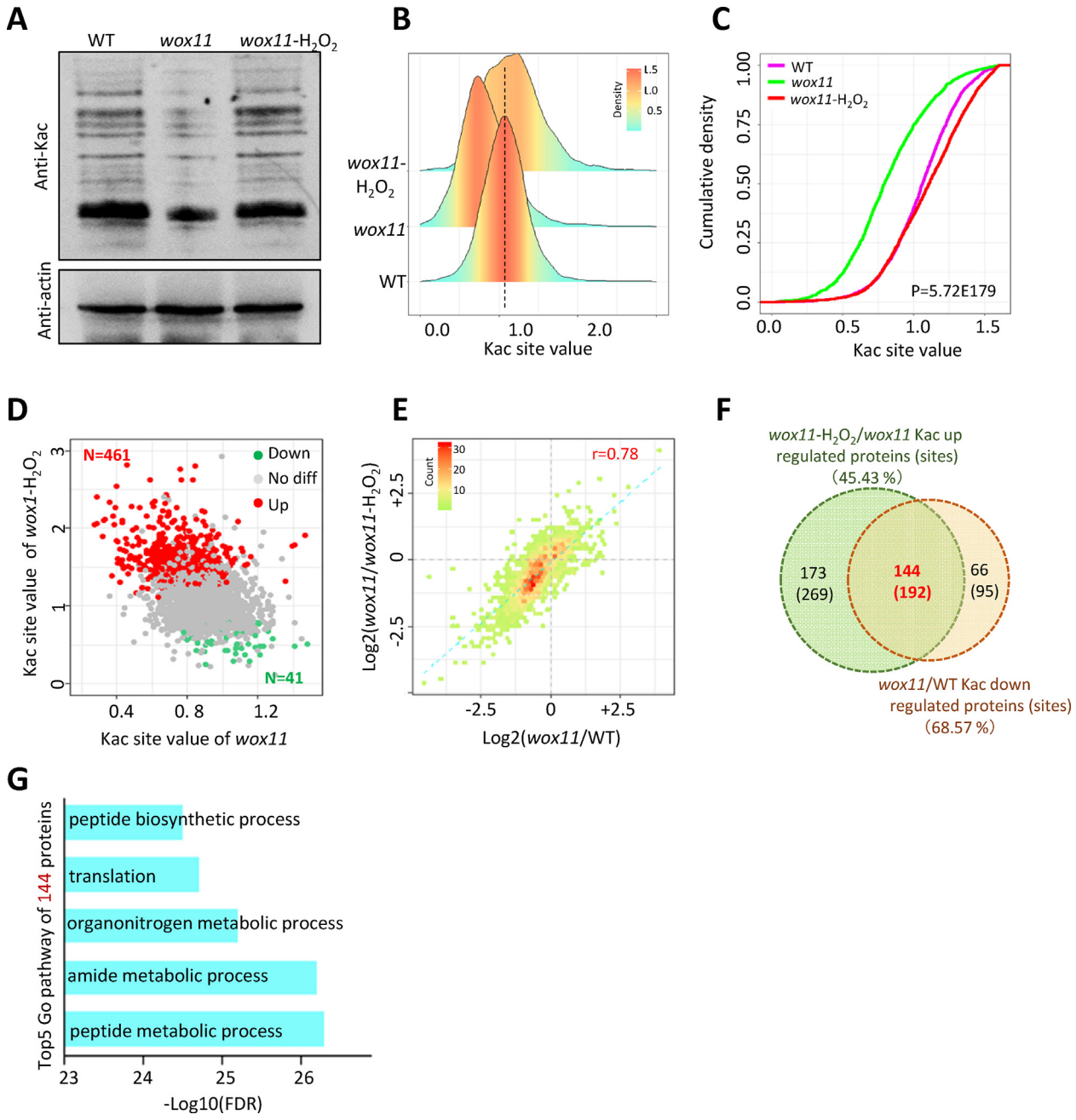

Fig. 5. H_2O_2 application restores Kac levels in *wox11* roots. (A) Immunoblotting detection of Kac levels with lysine acetylation antibody in crown roots of WT, *wox11* and *wox11*-H_2O_2. Immunoblotting with anti-actin antibody was used as loading control. **(B)** Ridge plots showing acetylation levels at individual Kac sites in WT, *wox11*-H_2O_2, and *wox11* crown roots. **(C)** Cumulative density plots of the acetylation levels at individual Kac sites in WT, *wox11*-H_2O_2, and *wox11* crown roots. P value between *wox11*-H_2O_2 and *wox11* was calculated by a two-tailed Student *t*-test. **(D)** Scattering plot of proteins with significantly upregulated (N = 461, fold change > 2) and downregulated (N = 41, fold change > 2) acetylation levels at individual Kac sites in *wox11*-H_2O_2 roots versus *wox11*. **(E)** Correlation between Kac changes in *wox11*/*wox11*-H_2O_2 and *wox11*/WT. Pearson correlation (r = 0.78) was shown. **(F)** Overlap between proteins (sites) with significant upregulated Kac levels in *wox11*-H_2O_2/*wox11* and proteins (sites) with significant downregulated Kac levels in *wox11*/WT. **(G)** GO pathway enrichment analysis of 144 overlapped proteins in F.

of the 2,645 identified proteins had more than one Kac site (Figure S5A, Supplementary Table S4). Most acetylated proteins were localized in the cytoplasm (Figure S5B). A comparison with the acetylomes of seeds [32], leaves [31], and embryos [30] revealed only 96 overlapping proteins, suggesting that different rice tissues/organs might have distinct protein acetylomes (Figure S5C). Motif analysis revealed that the flanking sequences of Kac sites were conserved in proteins in different subcellular compartments (Figure S5D). Acetylation levels at 287 Kac sites (13.63 %) showed > 2-fold decreases in *wox11* roots compared to WT, while only 47 Kac sites (2.23 %) showed > 2-fold increases in the mutant (Fig. 3B, C, Supplementary Table S5).

Protein hypo-acetylation is caused by lower H_2O_2 levels in wox11 roots

To investigate the relationship between ROS and protein Kac, we analyzed the overall acetylation level of proteins in WT roots treated with KI (WT-KI) by immunoblots. The analysis revealed significant decreases in the overall acetylation level of proteins in WT-KI compared to untreated control (WT) (Fig. 4A). Comparative

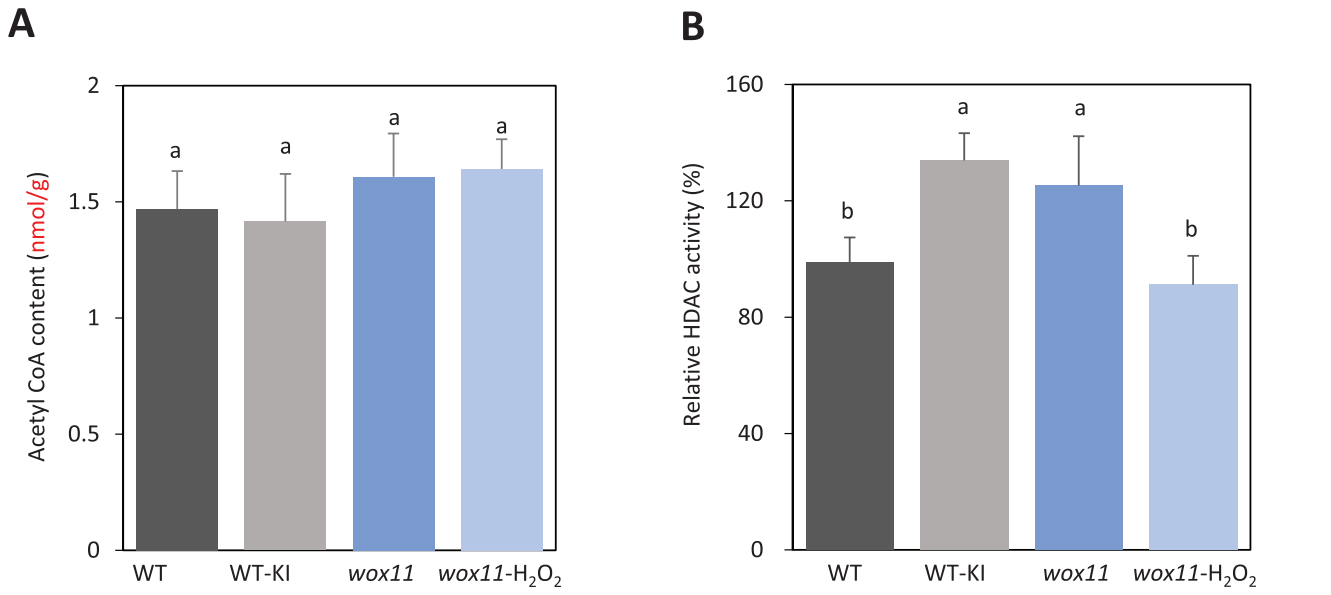

Fig. 6. Acetyl-CoA levels and HDAC activity in rice crown roots. (A) Changes in the levels of intracellular acetyl-CoA in crown roots of WT, WT-KI, *wox11*, and *wox11*-H_2O_2. Error bars were means ± SD (n = 3) from three biological replicates. **(B)** Tests of HDAC activities in WT, WT-KI, *wox11*, and *wox11* H_2O_2 crown roots. HDAC activities relative to WT (set at 100 %) were shown. Error bars were means ± SD (n = 3) from three biological replicates. Significance was calculated using one-way ANOVA with Tukey's multiple comparison tests. Different letters on the top of the bars indicate significant differences (P < 0.05), and the same letters on top of bars indicate no significant difference.

analysis of acetylproteomes also revealed an overall hypo-acetylation levels of proteins in WT-KI relative to WT roots (Fig. 4B, C). In WT-KI roots, 235 (10.88 %) Kac sites showed lower (> 2-fold) acetylation, while only 27 (1.25 %) sites displayed higher acetylation (> 2-fold) (Supplementary Table S6, Fig. 4D). Strikingly, the overall Kac levels in WT-KI and *wox11* roots were similar (Fig. 4E). There was no obvious difference in overall Kac level of proteins between WT-KI and *wox11* roots (Fig. 4F, Supplementary Table S7). Additionally, the changes in protein Kac levels between *wox11*/WT and WT-KI/WT were correlated (r = 0.73) (Fig. 4G). Indeed, 43.81 % (N = 92) of the proteins with downregulated Kac in *wox11* roots showed lower Kac levels in WT-KI roots (Fig. 4H), indicating that *wox11* mutation and KI application had a similar impact on protein acetylation level. These findings suggested that protein hypo-acetylation in *wox11* roots was caused by the decrease of H_2O_2. GO pathway enrichment analysis of the 92 (94) overlapped proteins (sites) revealed that the proteins were mostly enriched for the organonitrogen metabolic and peptide biosynthetic pathways (Fig. 4I).

H_2O_2 application restores protein Kac levels in wox11 roots

According to previous studies [12,38,39], application of a relatively low concentration of H_2O_2 (0.5 mM) could restore the H_2O_2 levels in *wox11* roots (Fig. 1C) and partially complemented *wox11* root phenotype (Fig. 1F). Immuno-blots and MS-based quantitative acetyl-proteomic analyses indicated that the protein Kac levels in *wox11* roots treated by H_2O_2 (*wox11*-H_2O_2) were restored to the WT levels (Fig. 5A-D). Furthermore, the changes of Kac levels in *wox11*/*wox11*-H_2O_2 were correlated (r = 0.78) with those in *wox11*/WT (Fig. 5E), and 68.57 % of proteins with hypo-Kac in *wox11* roots were restored to the WT levels after H_2O_2 treatment (Fig. 5F). The proteins with restored Kac levels in *wox11*-H_2O_2 showed the similar pathway enrichment to those with significantly decreased Kac in *wox11* and WT- KI roots (Fig. 4I, 5G). Together, these results indicated that Kac of proteins involved in protein synthesis and nitrogen metabolism are particularly controlled by cellular H_2O_2 levels in *wox11* roots.

Higher HDAC activity results in protein hypo-acetylation in wox11 roots

The protein hypo-acetylation detected in *wox11* roots seemed unrelated to the expression of histone deacetylase (HDAC)/histone acetyltransferase (HAT), because no obvious change of their mRNA and protein levels was observed in *wox11* transcriptomic and proteomic data or WT-KI root proteome (Figure S6A-C; Figure S7A, B). Previous studies suggested that redox may modulate protein acetylation by affecting acetyl-CoA accumulation [40,41]. However, the protein levels of acetyl-CoA biosynthetic and catabolic enzymes such as ACLA (ATP citrate lyase A), ACLAB (ATP citrate lyase B), ACS (acetyl-CoA synthase), and ACC (acetyl-CoA carboxylase) also displayed no change in *wox11* and WT-KI roots (Figure S7C, S8A, B). To examine the possibility that protein acetylation was caused by alteration of acetyl-CoA abundance, we measured acetyl-CoA in WT, WT-KI, *wox11*, and *wox11*-H_2O_2 root cells. The level of acetyl-CoA measured here was in line with previous reports in other plants [26,42], but no difference was observed in these plants (Fig. 6A).

As ROS can modulate HDACs activity [43,44], we therefore conducted a series of fluorescence-based HDAC enzyme activity assays. As shown in Fig. 6B, the activity of HDAC was significantly higher in *wox11* roots than in WT. Application of KI that reduces cellular H_2O_2 levels enhanced HDAC activity in WT roots (WT-KI), while application of H_2O_2 significantly attenuated HDAC activity in *wox11* roots (*wox11*- H_2O_2). These results suggested that the protein hypo-acetylation might be due to higher HDAC activity stimulated by the decreased ROS levels in *wox11* roots, though local fluctuation of acetyl-CoA on the dynamic changes of protein acetylation was not completely excluded.

HDAC oxidization might account for HDAC activity decrease

In order to identify specific HDACs that were regulated by ROS, thiol-modifying reagent 4-acetamido-4′ -maleimidylstilbene-2, 2′-disulfonic acid (AMS) was used to examine the redox state of rice HDAC SRT1, SRT2, HDA710, and HDA714, which have been functionally studied [38,33,34,45]. AMS could react with the reduced

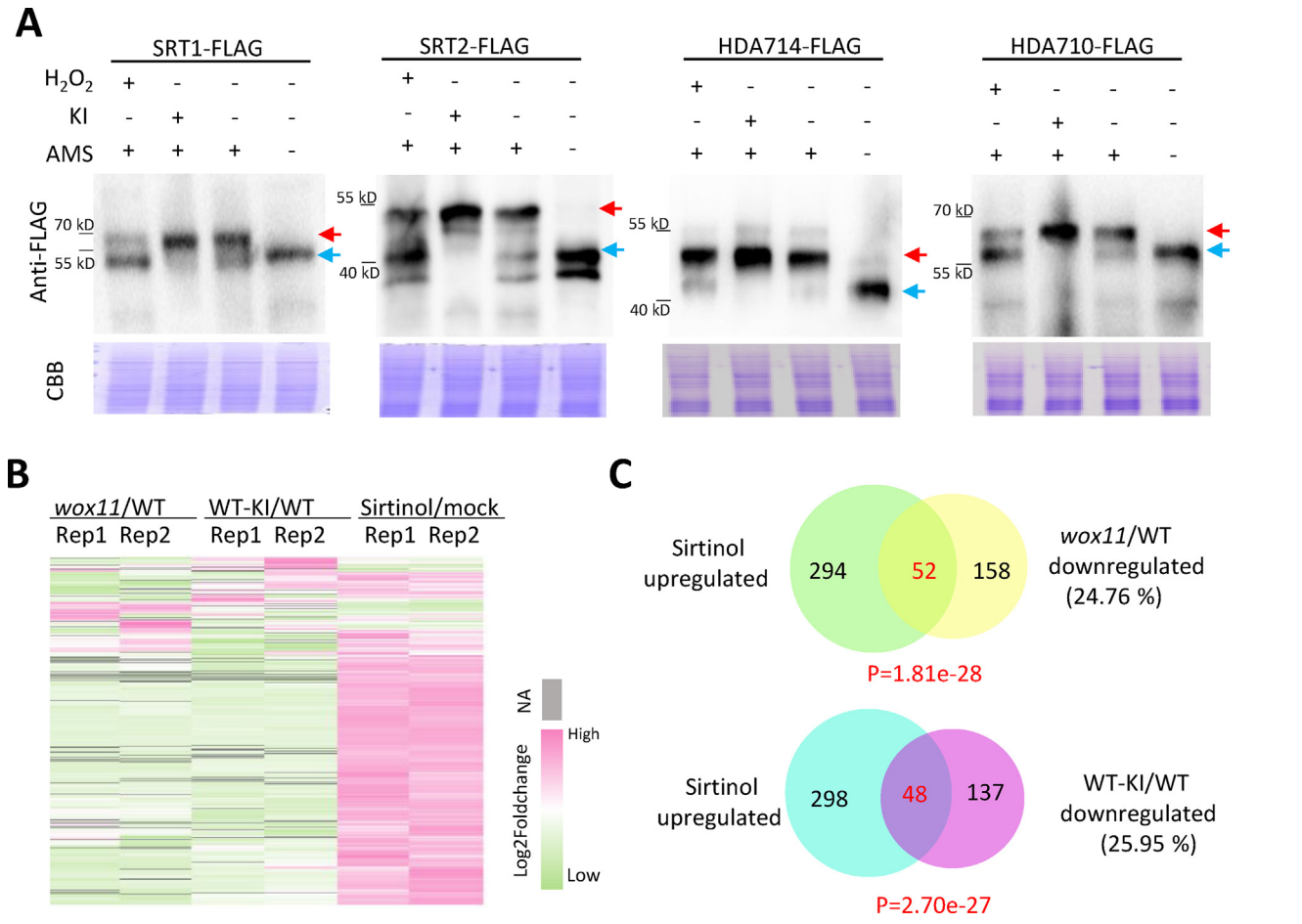

Fig. 7. Dynamic changes in protein Kac levels are regulated by redox-controlled HDAC activity. (A) Immunoblotting detection of redox status of SRT1-FLAG, SRT2-FLAG, HDA710-FLAG, and HDA714-FLAG proteins under KI or H_2O_2 treatments. The reduced cysteine was alkylated by the thiol-modifying agent AMS. Modification results in a shift of 0.5 kDa per modified cysteine residue. Proteins were separated by SDS-PAGE followed by immunoblotting with anti-FLAG antibody. Coomassie brilliant blue (CBB) was used as the loading control. When Western blotting, two replicates were performed. One replicate was used to detect protein amount by Coomassie brilliant blue staining, while another replicate was used to transfer to the membrane for Western blotting. Red and blue arrows indicate reduced and oxidized forms of HDACs, respectively. **(B)** Heatmap of changes of protein Kac levels in *wox11*/WT (*wox11* compared to WT), WT-KI/WT (WT-KI compared to WT) and sirtinol/mock (sirtinol treated plants compared to untreated controls). NA indicates that data is not available. **(C)** Upper: Venn diagram showing the overlap proteins with significantly upregulated Kac levels in sirtinol treated plants and significantly downregulated Kac levels in *wox11*. Lower: Venn diagram showing proteins with significantly upregulated Kac levels in sirtinol treated plants and proteins with clearly downregulated Kac levels in WT-KI. P values were calculated by Fisher's exact test.

cysteine and slow down the protein mobility on an SDS-PAGE gel, allowing the determination of protein redox status as a band shift [46,47]. To analyze the redox regulation of HDACs, overexpression lines (OE) fused with FLAG tag at C-terminal of SRT1, SRT2, HDA710, and HDA714 were analyzed under different redox treatments. The assays revealed that under normal conditions, a large fraction of the four HDAC proteins were all at a reduced state in these OE plants. KI addition further enhanced the reduced state of these HDACs. In contrast, the application of H_2O_2 led to the oxidization of a large fraction of SRT1, SRT2, HDA710, and, to a lesser extent, HDA714 in these OE plants (Fig. 7A). Based on the results, it is hypothesized that the four HDACs might be inactivated by H_2O_2 and contribute to protein hypo-acetylation in *wox11* mutant. To check the hypothesis, we tested the function of the rice NAD^+-dependent sirtuin family histone deacetylases SRT1 and SRT2 in protein acetylation by performing MS-based quantitative acetylproteomic analysis of WT plants treated with/or without sirtinol (a well-known specific inhibitor for sirtuin HDACs). The replicates showed good data reproducibility (Figure S9A, B). The inhibition of SRT1 and SRT2 activity indeed led to an obvious increase in Kac levels on many proteins (Figure S10A, B). In total, 681 Kac sites in 346 proteins displayed higher (> 1.5-fold) Kac in plants treated with sirtinol, while only 2 sites in 2 proteins displayed lower (> 1.5-fold) Kac levels (Figure S10C, D, Supplementary Table S8). Heatmap indicated that 70 % of the proteins with decreased Kac in *wox11* and WT-KI plants showed increased Kac in sirtinol-treated plants (Fig. 7B). In addition, 24.76 % (N = 52) and 25.95 % (N = 48) of the proteins with significantly reduced (> 2-fold) Kac levels in *wox11* and WT-KI showed up-regulation of Kac in sirtinol-treated plants, respectively (Fig. 7C). Collectively, these results suggested that HDAC activities mediated by redox state might contribute to hypo-acetylation of proteins in *wox11* roots.

Discussion

The CRs are the major component of root system in cereals, whose activity is strongly influenced by genetic factors and environmental conditions. Previous work showed that WOX11 controls CR development by regulating the expression of cytokinin and auxin signaling genes [16,17,48]. In this work, we identified a novel pathway of WOX11-controlled CR development in rice. We showed that ROS-related proteins are abundant in rice root cells and that WOX11 is required for the high expression levels of ROS-related genes and ROS (H_2O_2) accumulation in roots. This

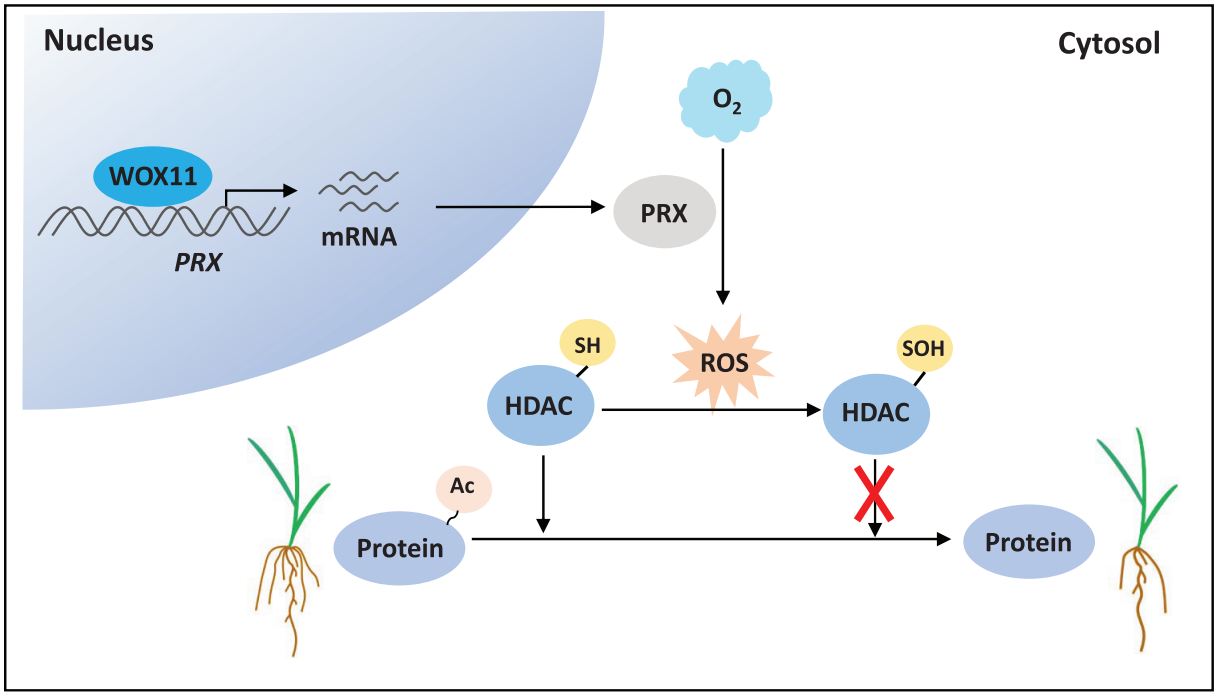

Fig. 8. A proposed model of WOX11, ROS signaling, and protein acetylation network regulating crown root development. WOX11 directly binds to and activates peroxidase (*PRX*) genes expression in crown roots (CRs). PRXs catalyze the formation of reactive oxygen species (ROS) in the cytosol of CR cells. Locally accumulated ROS oxidize histone deacetylases (HDAC) and inhibit their activities, thus leading to hyper-acetylation of proteins to promote CR growth.

developmentally-regulated ROS accumulation in roots stimulates protein lysine acetylation likely by inhibiting HDAC activities that can deacetylate both histones and non-histone proteins [49]. ROS-stimulated acetylation mainly targets proteins involved in nitrogen metabolism and protein synthesis, implying that activities of these pathways are critical for CR growth (Fig. 8). As cellular ROS level quickly changes in response to environmental cues, the ROS-regulated protein Kac might also respond to environmental condition to control CR growth and development in rice.

Protein acetylation modification may have central functions in regulating organogenesis

Post-translational modifications of proteins such as phosphorylation, ubiquitination, and SUMOylation increase the functional diversity of the proteome. In recent years, increasing evidence has shown that many proteins involved in metabolism, stress, development, and translation are acetylated [30,34,50,51]. For example, in rice, there are 297, 128, and 396 metabolism- and stress-related proteins modified by acetylation in seeds, embryos, and leaves, respectively [30,31,52]. Here, we detected 2,645 proteins with lysine acetylation sites in rice CRs, 908 of which have functions in metabolism- and stress-related pathways, about 7 times more than those detected in rice embryos (Figure S5C). Studies in yeast and animal cells suggest that the stoichiometry of protein Kac sites could help us to better evaluate the functionality of specific Kac site of a given protein [53,54]. This may be a direction for future research in the field of acetylation in rice. Anyway, our study highlights the importance of protein Kac in the root meristem. Although the role of Kac remains unknown for most of the acetylated proteins, recent results suggested that Kac of translational factors and ribosomal proteins may affect protein stability and translational efficiency in rice cells [34]. The observation that *wox11* mutation results in lower Kac but a higher accumulation of proteins of the protein synthesis pathway (Fig. 4I) suggested that ROS-controlled Kac may be related to protein synthesis activity in root cells.

WOX11 regulates PRX genes to control CR development

It was reported that PRX family proteins are involved in plant immunity and organogenesis by regulating ROS homeostasis [55–57]. For example, AtPRX71 negatively regulates cell growth and cell wall damage responses via the accumulation of H_2O_2 in the apoplast [58]. PRX17 regulates the development of lignified tissues in the process of vegetative to reproductive growth transition [59]. Additionally, the induced expression of *PRX* genes by fungi and bacteria [60] promotes the susceptibility of plants to these pathogens owing to the impaired cellular oxidative burst [61]. Our results showed that *PRX* loss-of-function decreases ROS levels and the CR number indicated that *PRX* plays a crucial role in maintaining high ROS levels critical for CR development (Fig. 2F, G, S3C). These results that demonstrated the roles of PRXs in root development are consistent with the previous reports in other plants [8,62]. Furthermore, our data showed that *PRX* genes are direct targets of WOX11 indicating that WOX11 controls CR development by directly activating ROS-related genes (Fig. 2A-E), in addition to regulating hormone signaling gene expression.

WOX11-mediated ROS levels modulate HDAC activities in root cells

Previous results showed that oxidative stress and NO accumulation inhibit the overall HDAC activities [63]. Our results showed that cellular ROS accumulation controlled by WOX11 could also affect HDACs activity (Fig. 6B). These results indicated that HDACs are sensitive to developmentally controlled ROS levels. Importantly, our data showed that the higher HDAC activities result in hypoacetylation, which is in agreement with the fact that several HDACs are localized in both nucleus and cytoplasm and deacetylate both histone and non-histone proteins in plants [49]. For instance, rice SRT1 deacetylates GAPDH and regulates its subcellu-

lar localization and moonlighting activity [38], while HDA714 is a cytoplasmic deacetylase required to maintain low acetylation of many non-histone proteins such as ribosomal proteins in rice cells [34]. The enrichment for protein synthesis pathways of hypo-acetylated proteins in *wox11* roots suggested that HDA714 may be one of the bona fide HDACs that respond to WOX11-controlled ROS levels to control acetylation of non-histone proteins in the cell [34]. Our data from the comparative acetyl-proteomics analysis suggested that WOX11-controlled ROS may at least partially affect SRT1 and SRT2 activities (Fig. 7B, C). Previous results showed that WOX11 promotes histone acetylation by recruiting the histone acetyltransferase GCN5-ADA2 complex at target loci [21]. The present results indicate that WOX11 can also stimulate histone acetylation by promoting ROS-mediated inhibition of HDACs which may be needed for the regulation of genes involved in CR development. Collectively, our finding establishes a new molecular pathway of WOX11-controlled CR development and highlights the molecular link between ROS and non-histone acetylation in CR development, although the underlying mechanisms remain to be elucidated. More importantly, the orchestration of ROS signaling and protein acetylation uncovers a new layer of redox regulation complexity and might play a crucial role in coordinating plant growth with environmental adaptation.

Compliance with ethics requirements.

This research work does not contain any studies with human or animal subjects.

Declaration of Competing Interest

The authors declare that they have no known competing financial interests or personal relationships that could have appeared to influence the work reported in this paper.

Acknowledgements

We thank Qinglu Zhang and Xianghua Li for technical assistance. This work was supported by grants from the National Natural Science Foundation of China (No. 31970806, 32100465, and 31730049), and the Postdoctoral Science Foundation of China (No. 2021M691183). We also thank for the support of BaiChuan Fellowship of College of Life Science and Technology, Huazhong Agricultural University.

Appendix A. Supplementary material

Supplementary data to this article can be found online at https://doi.org/10.1016/j.jare.2022.07.010.

References

[1] Finkel T. Signal transduction by reactive oxygen species. J Cell Biol 2011;194:7–15. doi: https://doi.org/10.1083/jcb.201102095.
[2] Schieber M, Chandel N. ROS function in redox signaling and oxidative stress. Curr Biol 2014;24(10):R453–62. doi: https://doi.org/10.1016/j.cub.2014.03.034.
[3] Waszczak C, Carmody M, Kangasjärvi J. Reactive oxygen species in plant signaling. Annu Rev Plant Biol 2018;69(1):209–36. doi: https://doi.org/10.1146/annurev-arplant-042817-040322.
[4] Huang H, Ullah F, Zhou DX, Yi M, Zhao Y. Mechanisms of ROS regulation of plant development and stress responses. Front Plant Sci 2019;10:800. doi: https://doi.org/10.3389/fpls.2019.00800.
[5] Zhou H, Zhang F, Zhai F, Su Ye, Zhou Y, Ge Z, et al. Rice GLUTATHIONE PEROXIDASE1-mediated oxidation of bZIP68 positively regulates ABA-independent osmotic stress signaling. Mol Plant 2022;15(4):651–70. doi: https://doi.org/10.1016/j.molp.2021.11.006.
[6] Yang RS, Xu F, Wang YM, Zhong WS, Dong L, Shi YN, et al. Glutaredoxins regulate maize inflorescence meristem development via redox control of TGA transcriptional activity. Nat Plants 2021;7(12):1589–601. doi: https://doi.org/10.1038/s41477-021-01029-2.
[7] Huang X, Chen S, Li W, Tang L, Zhang Y, Yang N, et al. ROS regulated reversible protein phase separation synchronizes plant flowering. Nat Chem Biol 2021;17(5):549–57. doi: https://doi.org/10.1038/s41589-021-00739-0.
[8] Tsukagoshi H, Busch W, Benfey PN. Transcriptional regulation of ros controls transition from proliferation to differentiation in the root. Cell 2010;143(4):606–16. doi: https://doi.org/10.1016/j.cell.2010.10.020.
[9] Yu Q, Tian H, Yue K, Liu J, Zhang B, Li X, et al. A P-Loop NTPase regulates quiescent center cell division and distal stem cell identity through the regulation of ROS homeostasis in Arabidopsis root. PLoS Genet 2016;12(9):e1006175. doi: https://doi.org/10.1371/journal.pgen.1006175.
[10] Yamada M, Han X, Benfey PN. RGF1 controls root meristem size through ROS signalling. Nature 2020;577(7788):85–8. doi: https://doi.org/10.1038/s41586-019-1819-6.
[11] Yu X, Pasternak T, Eiblmeier M, Ditengou F, Kochersperger P, Sun J, et al. Plastid-localized glutathione reductase2–regulated glutathione redox status is essential for Arabidopsis root apical meristem maintenance. Plant Cell 2013;25(11):4451–68. doi: https://doi.org/10.1105/tpc.113.117028.
[12] Xu L, Zhao H, Ruan W, Deng M, Wang F, Peng J, et al. ABNORMAL INFLORESCENCE MERISTEM1 functions in salicylic acid biosynthesis to maintain proper reactive oxygen species levels for root meristem activity in rice. Plant Cell 2017;29(3):560–74. doi: https://doi.org/10.1105/tpc.16.00665.
[13] Suzuki N, Koussevitzky S, Mittler R, Miller G. ROS and redox signalling in the response of plants to abiotic stress. Plant Cell Environ 2012;35:259–70. doi: https://doi.org/10.1111/j.1365-3040.2011.02336.x.
[14] Krieger G, Shkolnik D, Miller G, Fromm H. Reactive oxygen species tune root tropic responses. Plant Physiol 2016;172:1209–20. doi: https://doi.org/10.1104/pp.16.00660.
[15] Pardo-Hernández M, López-Delacalle M, Rivero RM. ROS and NO regulation by melatonin under abiotic stress in plants. Antioxidants 2020;9:1078. doi: https://doi.org/10.3390/antiox9111078.
[16] Zhao Y, Hu Y, Dai M, Huang L, Zhou DX. The WUSCHEL-related homeobox gene WOX11 is required to activate shoot-borne crown root development in rice. Plant Cell 2009;21:736–48. doi: https://doi.org/10.1105/tpc.108.061655.
[17] Zhao Yu, Cheng S, Song Y, Huang Y, Zhou S, Liu X, et al. The interaction between rice ERF3 and WOX11 promotes crown root development by regulating gene expression involved in cytokinin signaling. Plant Cell 2015;27(9):2469–83. doi: https://doi.org/10.1105/tpc.15.00227.
[18] Cheng S, Zhou D-X, Zhao Yu. WUSCHEL-related homeobox gene WOX11 increases rice drought resistance by controlling root hair formation and root system development. Plant Signal Behav 2016;11(2):e1130198. doi: https://doi.org/10.1080/15592324.2015.1130198.
[19] Chen G, Feng H, Hu Q, Qu H, Chen A, Yu L, et al. Improving rice tolerance to potassium deficiency by enhancing OsHAK16p:WOX11-controlled root development. Plant Biotechnol J 2015;13(6):833–48. doi: https://doi.org/10.1111/pbi.12320.
[20] Li X, Guo Z, Lv Y, Cen X, Ding X, Wu H, et al. Genetic control of the root system in rice under normal and drought stress conditions by genome-wide association study. PLoS Genet 2017;13(7):e1006889. doi: https://doi.org/10.1371/journal.pgen.1006889.
[21] Zhou S, Jiang W, Long F, Cheng S, Yang W, Zhao Yu, et al. Rice homeodomain protein WOX11 recruits a histone acetyltransferase complex to establish programs of cell proliferation of crown root meristem. Plant Cell 2017;29(5):1088–104. doi: https://doi.org/10.1105/tpc.16.00908.
[22] Jiang W, Zhou S, Zhang Q, Song H, Zhou DX, Zhao Y. Transcriptional regulatory network of WOX11 is involved in the control of crown root development, cytokinin signals, and redox in rice. J Exp Bot 2017;68:2787–98. doi: https://doi.org/10.1093/jxb/erx153.
[23] He Y, Zhang T, Yang N, Xu M, Yan L, Wang L, et al. Self-cleaving ribozymes enable the production of guide RNAs from unlimited choices of promoters for CRISPR/Cas9 mediated genome editing. J Genet Genomics 2017;44(9):469–72. doi: https://doi.org/10.1016/j.jgg.2017.08.003.
[24] Lei Y, Lu Li, Liu H-Y, Li S, Xing F, Chen L-L. CRISPR-P: a web tool for synthetic single-guide RNA design of CRISPR-system in plants. Mol Plant 2014;7(9):1494–6. doi: https://doi.org/10.1093/mp/ssu044.
[25] Gibson DG, Young L, Chuang R-Y, Venter JC, Hutchison CA, Smith HO. Enzymatic assembly of DNA molecules up to several hundred kilobases. Nat Methods 2009;6(5):343–5.
[26] Zhao H, Zhong S, Sang L, Zhang X, Chen Z, Wei's Q, et al. PaACL silencing accelerates flower senescence and changes the proteome to maintain metabolic homeostasis in Petunia hybrida. J Exp Bot 2020;71(16):4858–76. doi: https://doi.org/10.1093/jxb/eraa208.
[27] Yoshida K, Hisabori T. Simple method to determine protein redox state in Arabidopsis thaliana. BIO-PROTOCOL 2019;9:. doi: https://doi.org/10.21769/BioProtoc.3250e3250.
[28] Topf U, Suppanz I, Samluk L, Wrobel L, Böser A, Sakowska P, et al. Quantitative proteomics identifies redox switches for global translation modulation by mitochondrially produced reactive oxygen species. Nat Commun 2018;9(1). doi: https://doi.org/10.1038/s41467-017-02694-8.
[29] Cheng S, Tan F, Lu Y, Liu X, Li T, Yuan W, et al. WOX11 recruits a histone H3K27me3 demethylase to promote gene expression during shoot development in rice. Nucleic Acids Res 2018;46(5):2356–69. doi: https://doi.org/10.1093/nar/gky017.
[30] He D, Wang Q, Li M, Damaris RN, Yi X, Cheng Z, et al. Global proteome analyses of lysine acetylation and succinylation reveal the widespread involvement of both modification in metabolism in the embryo of germinating rice seed. J Proteome Res 2016;15(3):879–90. doi: https://doi.org/10.1021/acs.

jproteome.5b0080510.1021/acs.jproteome.5b00805.s00110.1021/acs.jproteome.5b00805.s002.
[31] Zhou H, Finkemeier I, Guan W, Tossounian M-A, Wei Bo, Young D, et al. Oxidative stress-triggered interactions between the succinyl- and acetyl-proteomes of rice leaves. Plant Cell Environ 2018;41(5):1139–53.
[32] Xue C, Liu S, Chen C, Zhu J, Yang X, Zhou Y, et al. Global proteome analysis links lysine acetylation to diverse functions in Oryza Sativa. Proteomics 2018;18 (1):1700036. doi: https://doi.org/10.1002/pmic.201700036.
[33] Lu Y, Xu Q, Liu Y, Yu Y, Cheng Z-Y, Zhao Yu, et al. Dynamics and functional interplay of histone lysine butyrylation, crotonylation, and acetylation in rice under starvation and submergence. Genome Biol 2018;19(1). doi: https://doi.org/10.1186/s13059-018-1533-y.
[34] Xu Q, Liu Q, Chen Z, Yue Y, Liu Y, Zhao Yu, et al. Histone deacetylases control lysine acetylation of ribosomal proteins in rice. Nucleic Acids Res 2021;49 (8):4613–28. doi: https://doi.org/10.1093/nar/gkab244.
[35] T. Tian, Y. Liu, H. Yan, Q. You, X. Yi, Z. Du, et al., agriGO v2.0: a GO analysis toolkit for the agricultural community, 2017 update, Nucleic Acids Res 45 (2017) W122-W129. doi: 10.1093/nar/gkx382.
[36] Chen C, Chen H, Zhang Yi, Thomas HR, Frank MH, He Y, et al. TBtools: an integrative toolkit developed for interactive analyses of big biological data. Mol Plant 2020;13(8):1194–202. doi: https://doi.org/10.1016/j.molp.2020.06.009.
[37] Colaert N, Helsens K, Martens L, Vandekerckhove J, Gevaert K. Improved visualization of protein consensus sequences by iceLogo. Nat Methods 2009;6 (11):786–7. doi: https://doi.org/10.1038/nmeth1109-786.
[38] Zhang H, Zhao Y, Zhou DX. Rice NAD+-dependent histone deacetylase OsSRT1 represses glycolysis and regulates the moonlighting function of GAPDH as a transcriptional activator of glycolytic genes. Nucleic Acids Res 2017;45:12241–55. doi: https://doi.org/10.1093/nar/gkx825.
[39] Chen J, Li H, Yang K, Wang Y, Yang L, Hu L, et al. Melatonin facilitates lateral root development by coordinating PAO-derived hydrogen peroxide and Rboh-derived superoxide radical. Free Radic Biol Med 2019;143:534–44. doi: https://doi.org/10.1016/j.freeradbiomed.2019.09.011.
[40] Ojima Y, Suryadarma P, Tsuchida K, Taya M. Accumulation of pyruvate by changing the redox status in Escherichia coli. Biotechnol Lett 2012;34 (5):889–93. doi: https://doi.org/10.1007/s10529-011-0842-y.
[41] R. m. SK, Wang Y, Zhang X, Cheng H, Sun L, He S, et al. Redox components: key regulators of epigenetic modifications in plants. Int J Mol Sci 2020;21(4):1419. doi: https://doi.org/10.3390/ijms21041419.
[42] Tumaney AW, Ohlrogge JB, Pollard M. Acetyl coenzyme A concentrations in plant tissues. J Plant Physiol 2004;161(4):485–8. doi: https://doi.org/10.1078/0176-1617-01258.
[43] Jänsch N, Meyners C, Muth M, Kopranovic A, Witt O, Oehme I, et al. The enzyme activity of histone deacetylase 8 is modulated by a redox-switch. Redox Biol 2019;20:60–7. doi: https://doi.org/10.1016/j.redox.2018.09.013.
[44] Ago T, Liu T, Zhai P, Chen W, Li H, Molkentin JD, et al. A redox-dependent pathway for regulating class II HDACs and cardiac hypertrophy. Cell 2008;133 (6):978–93. doi: https://doi.org/10.1016/j.cell.2008.04.041.
[45] Ullah F, Xu Q, Zhao Yu, Zhou D-X. Histone deacetylase HDA710 controls salt tolerance by regulating ABA signaling in rice. J Integr Plant Biol 2021;63 (3):451–67. doi: https://doi.org/10.1111/jipb.13042.
[46] Frand AR, Kaiser CA. The ERO1 gene of yeast is required for oxidation of protein dithiols in the endoplasmic reticulum. Mol Cell 1998;1(2):161–70.
[47] Yoshida K, Hisabori T. Determining the rate-limiting step for light-responsive redox regulation in chloroplasts. Antioxidants 2018;7(11):153. doi: https://doi.org/10.3390/antiox7110153.
[48] Zhang T, Li R, Xing J, Yan L, Wang R, Zhao Y. The YUCCA-Auxin-WOX11 module controls crown root development in rice. Front Plant Sci 2018;9. doi: https://doi.org/10.3389/fpls.2018.00523.
[49] Shen Y, Wei W, Zhou D-X. Histone acetylation enzymes coordinate metabolism and gene expression. Trends Plant Sci 2015;20(10):614–21. doi: https://doi.org/10.1016/j.tplants.2015.07.005.
[50] Hartl M, Füßl M, Boersema PJ, Jost J-O, Kramer K, Bakirbas A, et al. Lysine acetylome profiling uncovers novel histone deacetylase substrate proteins in Arabidopsis. Mol Syst Biol 2017;13(10):949.
[51] M. Hartl, A.-C. König, I. Finkemeier, Identification of lysine-acetylated mitochondrial proteins and their acetylation sites, Plant Mitochondria: Methods and Protocols, J. Whelan and M. W. Murcha, 2015, Springer New York, New York, NY, 107-121.
[52] Wang Y, Hou Y, Qiu J, Li Z, Zhao J, Tong X, et al. A quantitative acetylomic analysis of early seed development in rice (Oryza sativa L.). Int J Mol Sci 2017;18(7):1376. doi: https://doi.org/10.3390/ijms18071376.
[53] Weinert BT, Iesmantavicius V, Moustafa T, Scholz C, Wagner SA, Magnes C, et al. Acetylation dynamics and stoichiometry in Saccharomyces cerevisiae. Mol Syst Biol 2014;10:716. doi: https://doi.org/10.1002/msb.134766.
[54] Hansen BK, Gupta R, Baldus L, Lyon D, Narita T, Lammers M, et al. Analysis of human acetylation stoichiometry defines mechanistic constraints on protein regulation. Nat Commun 2019;10(1). doi: https://doi.org/10.1038/s41467-019-09024-0.
[55] Lu D, Wang T, Persson S, Mueller-Roeber B, Schippers JH. Transcriptional control of ROS homeostasis by KUODA1 regulates cell expansion during leaf development. Nat Commun 2014;5:3767. doi: https://doi.org/10.1038/ncomms4767.
[56] Passardi F, Penel C, Dunand C. Performing the paradoxical: how plant peroxidases modify the cell wall. Trends Plant Sci 2004;9(11):534–40. doi: https://doi.org/10.1016/j.tplants.2004.09.002.
[57] Valério L, De Meyer M, Penel C, Dunand C. Expression analysis of the Arabidopsis peroxidase multigenic family. Phytochemistry 2004;65 (10):1331–42. doi: https://doi.org/10.1016/j.phytochem.2004.04.017.
[58] Raggi S, Ferrarini A, Delledonne M, Dunand C, Ranocha P, De Lorenzo G, et al. The Arabidopsis class III peroxidase AtPRX71 negatively regulates growth under physiological conditions and in response to cell wall damage. Plant Physiol 2015;169:2513–25. doi: https://doi.org/10.1104/pp.15.01464.
[59] Cosio C, Ranocha P, Francoz E, Burlat V, Zheng Y, Perry SE, et al. The class III peroxidase PRX17 is a direct target of the MADS-box transcription factor AGAMOUS-LIKE15 (AGL15) and participates in lignified tissue formation. New Phytol 2017;213:250–63. doi: https://doi.org/10.1111/nph.14127.
[60] Shigeto J, Tsutsumi Y. Diverse functions and reactions of class III peroxidases. New Phytol 2016;209:1395–402. doi: https://doi.org/10.1111/nph.13738.
[61] Daudi A, Cheng Z, O'Brien JA, Mammarella N, Khan S, Ausubel FM, et al. The apoplastic oxidative burst peroxidase in arabidopsis is a major component of pattern-triggered immunity. Plant Cell 2012;24(1):275–87. doi: https://doi.org/10.1105/tpc.111.093039.
[62] Mabuchi K, Maki H, Itaya T, Suzuki T, Nomoto M, Sakaoka S, et al. MYB30 links ROS signaling, root cell elongation, and plant immune responses. Proc Natl Acad Sci U S A 2018;115(20). doi: https://doi.org/10.1073/pnas.1804233115.
[63] Mengel A, Ageeva A, Georgii E, Bernhardt J, Wu K, Durner J, et al. Nitric oxide modulates histone acetylation at stress genes by inhibition of histone deacetylases. Plant Physiol 2017;173(2):1434–52. doi: https://doi.org/10.1104/pp.16.01734.